Photo-active bimetallic and trimetallic nanocomposites in conjugation with macromolecules

R. Ostruzska[1], V. Svačinová[1], M. Petr[2], K. Šišková[1,*]

[1] Department of Experimental Physics, Faculty of Science, Palacký University Olomouc, 17. Listopadu 12, 771 46 Olomouc, Czech Republic
[2] CATRIN, Palacký University Olomouc, Šlechtitelů 27, 779 00 Olomouc, Czech Republic
karolina.siskova@upol.cz ; Tel. +420 585 634 291

V. Lacmanová[3], P. Slepička[3], F. Průša[4], O. Kvítek[3], A. Kutová[3], A. Řezníčková[3,*]

[3] Department of Solid State Engineering, University of Chemistry and Technology Prague, 166 28 Prague, Czech Republic
[4] Department of Metals and Corrosion Engineering, University of Chemistry and Technology Prague, 166 28 Prague, Czech Republic
alena.reznickova@vscht.cz ; Tel. +420 220 445 158

Abstract

Increasing microbial resistance requires finding new effective antibacterial agents. Bimetallic and trimetallic nanocomposites containing Au or AuAg nanostructures and superparamagnetic iron oxide nanoparticles (SPIONs) can represent an efficient tool to inhibit bacterial growth. Silver is well-known for its antobacterial effect; while SPIONs for OH radical generation when exposed to UV radiation, as we demonstrated in our previous work (1). Therefore, the antibacterial activity of nanocomposite can be controlled by on/off UV light switching. The bi/trimetallic nanocomposite was grafted on surface modified plasma-treated polyethylene terephthalate (PET) substrate via the chemical bond formation between Au/AuAg nanostructures and biphenyldithiol (BPD), similarly as in (2). The final devices (*AuNC-BSA-SPION@PET-pl-BPD* and *AuAgNC-BSA-SPION@PET-pl-BPD*) were characterized using several spectroscopic and microscopic techniques. The antibacterial test against *Escherichia Coli* (*E. Coli*), without and with UVA light irradiation, confirms the successful applicability of the final devices: when no UVA light applied, the antibacterial effect of trimetallic sample was observed solely (not for bimetallic one); on the other hand, using UVA light (365 nm) exposure, the bacterial growth inhibition was observed for both, *AuNC-BSA-SPION@PET-pl-BPD* and *AuAgNC-BSA-SPION@PET-pl-BPD*.

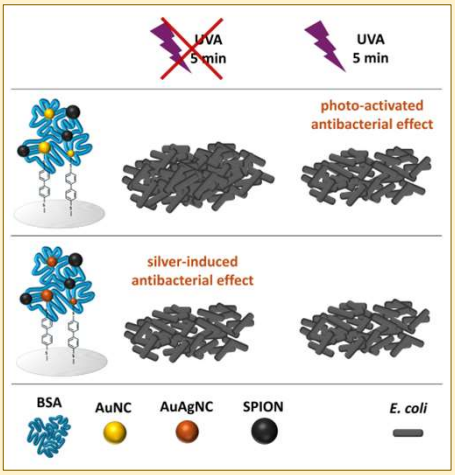

Elemental composition determined using X-ray photoelectron spectroscopy (XPS)

Table 1 : Comparison of the elemental composition of *AuNC-BSA-SPION@PET-pl-BPD* and) *AuAgNC-BSA-SPION@PET-pl BPD* determined for subsurface (0°) and top (81°) layers.

Element	AuNC-BSA-SPION@PET-pl-BPD		AuAgNC-BSA-SPION@PET-pl-BPD	
	Subsurface layers (0°) (Atomic %)	Top layers (81°) (Atomic %)	Subsurface layers (0°) (Atomic %)	Top layers (81°) (Atomic %)
C (1s)	66.0	67.2	62.6	63.1
O (1s)	22.3	22.1	24.8	25.1
N (1s)	8.1	7.2	8.5	7.7
S (2p)	1.5	1.4	1.5	1.1
Fe (2p)	2.1	2.1	2.1	2.7
Au (3d)	< 0.1	< 0.1	0.1	0.1
Ag (4f)	-	-	0.3	0.2

Sample preparation

PET (polyethyleneterephthalate) substrate was activated in DC Ar^+ plasma device, then the samples were immersed into methanol-based solution of BPD (biphenyl - 4,4´- dithiol) for 24 hours. Afterwards, they were transferred into the aqueous solution of bimetallic (*AuNC-BSA-SPION*) or trimetallic (*AuAgNC-BSA-SPION*) nanocomposites (syntheses are described in (3) and (4) in details).

Sample surface analysis using AFM

Grafting bi/trimetallic nanocomposites on pl-BPD-PET substrate leads towards a surface roughness increase as determined for the final device. Morphology of the surface structures of the final device seem to be globular, rounded, without presence of any sharp crystals and/or edges. Consequently, it could be suitable for cell adhesion. In fact, surface roughness represents one of the factors influencing adhesion of cells in general and bacteria in particular.

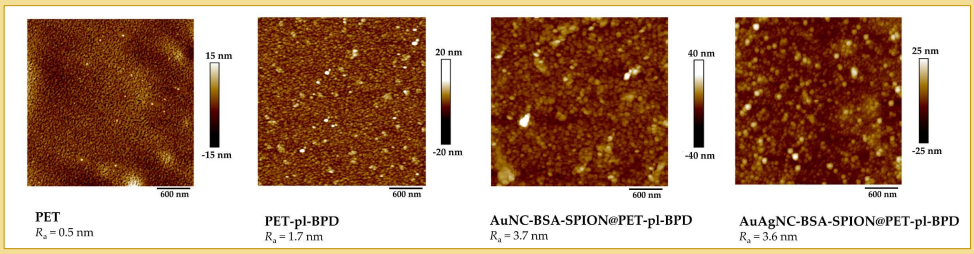

Figure 1: Atomic force microscopic (AFM) images of PET substrate (*PET*), plasma-treated BPD modified PET substrate (*PET-pl-BPD*), and plasma-treated BPD modified PET substrate with grafted bimetallic (*AuNC-BSA-SPION@PET-pl-BPD*) and trimetallic (*AuAgNC-BSA-SPION@PET-pl-BPD*) nanocomposite. Surface roughness values (R_a) determined for 3 × 3 μm² are given.

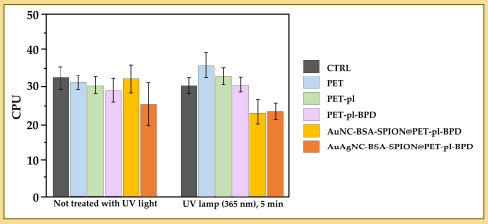

Figure 2: Antibacterial effect against *Escherichia coli* . Results of antibacterial testing of PET substrate (*PET*), plasma-treated PET substrate (*PET-pl*), plasma-treated BPD modified PET substrate (*PET-pl-BPD*), and plasma-treated BPD modified PET substrate with grafted bimetallic (*AuNC-BSA-SPION@PET-pl-BPD*) and trimetallic (*AuAgNC-BSA-SPION@PET-pl-BPD*) nanocomposite. As a control (*CTRL*), bacterial suspension was dropped on the bottom of a sterile Petri dish. Colony producing units (*CPU*) are expressed on y axis.

Antibacterial activity testing

Potential antibacterial properties of final devices were investigated employing drop plate methods against *Escherichia coli*. *AuAgNC-BSA-SPION@PET-pl-BPD* exhibits a slight antibacterial effect due to the presence of silver, whereas this effect was not observed for *AuNC-BSA-SPION@PET-pl-BPD* (left part). Exposure to UVA light (right part) leads to a statistically significant photo-activated antibacterial activity of *AuNC-BSA-SPION@PET-pl-BPD*, most probably owing to OH· radical production induced by UVA-light irradiation of SPIONs.

Conclusion

Bi/trimetallic nanocomposites consisting of Au or AuAg nanoclusters and SPIONs were successfully grafted on modified PET substrate. Spectroscopic characterization (survey and detailed XPS scans) proved that bi/trimetallic nanocomposites are covalently attached via Au-S bond to the BPD-modified PET substrate. AFM confirmed tha surface roughness increase of the final devices in comparison to the substrate. Antibacterial activity against *E. coli* was observed for *AuAgNC-BSA-SPION@PET-pl-BPD*, whereas UVA-light-induced antibacterial aktivity for *AuNC-BSA-SPION@PET-pl-BPD*. Therefore, bacterial growth was inhibited by the presence of silver and/or by the production of OH· radicals generated by UVA irradiation.

Acknowledgement:
This research was funded by the Czech Science Foundation, grant no. 25-15590S, and by Internal Grant Agency of Palacký University, grants no. IGA_PřF_2024_002 and no. IGA_PřF_2025_007.

References:
(1) G. Zoppellaro, R. Ostruszka, K. Sisková, Engineered protein-iron and/or gold-protein-iron nanocomposites in agueous solutions upon UVA light: Photo-iduced electron transfer possibilities and limitation, Journal of Photochemistry & Photobiology, A: Chemistry 450 (2024) 115415. https://doi.org/10.1016/j.jphotochem.2023.115415.
(2) V. Švorčík, Z. Kolská, O. Kvítek, J. Siegel, A. Řezníčková, P. Řezanka, K. Záruba, "Soft and Rigid" dithiols and Au nanoparticles grafteing on plasma-terated polyethyleneterephthalate, Nanoscale Res Lett. 6 (2011) 1–7. https://doi.org/10.1186/1556-276X-6-607.
(3) R. Ostruszka, A. Halili, T. Pluháček, L. Rárová, D. Jirák, K. Šišková, Advanced protein-embedded bimetallic nanocomposite optimalized for *in vivo* fluorescence and magnetic resonance bimodal imaging, Journal of Colloid and Interface Science. 663 (2024) 467–477. https://doi.org/10.1016/j.jcis.2024.02.116.
(4) V. Svačinová, A. Halili, R. Ostruszka, T. Pluháček, K. Jiráková, D. Jirák, K. Šišková, Trimetallic nanocomposites developed for efficient in vivo bimodal imaging via fluorescence and magnetic resonance, J. Mater. Chem. B 12 (2024) 8153–8166. https://doi.org/10.1039/D4TB00655K.